Scientific Research Publishing

Journal of Applied Mathematics and Physics, 2025, 13(3), 857-870
https://www.scirp.org/journal/jamp
ISSN Online: 2327-4379
ISSN Print: 2327-4352

Breather Solutions and Their Transformation Mechanisms of the (2 + 1)-Dimensional Boiti-Leon-Manna-Pempinelli Equation

Xingqi Xiao

College of Science, University of Shanghai for Science and Technology, Shanghai, China
Email: 1449504351@qq.com

How to cite this paper: Xiao, X.Q. (2025) Breather Solutions and Their Transformation Mechanisms of the (2 + 1)-Dimensional Boiti-Leon-Manna-Pempinelli Equation. *Journal of Applied Mathematics and Physics*, **13**, 857-870.
https://doi.org/10.4236/jamp.2025.133045

Received: March 1, 2025
Accepted: March 21, 2025
Published: March 24, 2025

Abstract

In this paper, we investigate the transformation phenomenon of the first-order breather and the second-order breather. First, we obtain the 2-solitary wave and 4-solitary wave solutions of the (2 + 1)-dimensional Boiti-Leon-Manna-Pempinelli (BLMP) equation by using the Hirota bilinear method. Then by analyzing and controlling characteristic lines, we derive several types of nonlinear transformantion waves and give the corresponding figures.

Keywords

Hirota Bilinear Method, The (2 + 1)-Dimensional Boiti-Leon-Manna-Pempinelli Equation, Characteristic Line, Breather

1. Introduction

With the development of technology, linear equations are often insufficient in fully capturing the complexity and intricacies of natural phenomena. As a result, nonlinear partial differential equations (NLPDEs) have emerged as essential models for describing intricate behaviors in nature. The study of soliton equation is an important direction dedicated to uncovering the nonlinear phenomena, which originates from many fields such as applied physics, life sciences, oceanography and other fields [1] [2] [3] [4].

Recently, the study of solitary wave solutions of the soliton equation has been a focus and many methods have been developed, such as the Darboux transform method [5] [6], the inverse scattering method [7] [8], the Hirota bilinear method [9] [10] [11] [12], tanh-function method [13], ansatz method [14] and other approaches [15]. The Hirota method used in this paper is a powerful and effective

tool to investigate the exact solutions of NLPDEs. The (2 + 1)-dimensional Boiti-Leon-Manna-Pempinelli (BLMP) equation was initially derived through the study of the weak Lax pair associated with the KdV equation [16]. Originally, this equation was introduced to describe nonlinear wave phenomena and shock wave propagation in incompressible fluids. Beyond fluid mechanics, the BLMP equation has also been widely applied in wave analysis within optical fiber communications, plasma physics, and solid mechanics. Many studies have been carried out on solving the exact solutions of the (2 + 1) and (3 + 1)-dimensional BLMP equations and structures of their solutions [17] [18] [19] [20] [21] by using different methods.

In this paper, we study the (2 + 1)-dimensional BLMP equation

$$u_{xxxy} + u_{yt} - 3u_{xx}u_y - 3u_x u_{xy} = 0, \tag{1.1}$$

where $u = u(x, y, t)$ is a function of x, y and t. Through the transformation [22] with a parameter u_0

$$u = -2\left[\ln f\right]_x + u_0 y, \tag{1.2}$$

the (2 + 1)-dimensional BLMP equation can be rewritten as the following Hirota bilinear form

$$\left(D_y D_t + D_y D_x^3 - 3u_0 D_x^2\right) f \cdot f = 0, \tag{1.3}$$

where

$$\begin{aligned} &D_x^m D_y^n D_t^p f \cdot g \\ &= \left(\partial_x - \partial_{x'}\right)^m \left(\partial_y - \partial_{y'}\right)^n \left(\partial_t - \partial_{t'}\right)^p f(x, y, t) g(x', y', t')\big|_{x'=x, y'=y, t'=t}. \end{aligned} \tag{1.4}$$

For soliton equations, exact solutions include solitary wave solutions, breather solutions, lump solutions [23] [24], etc. A solitary wave that exhibits periodic oscillations within a certain region, resembling a breathing motion, is defined as a breather [25]. Some researchers have discovered that transformations can occur between different types of nonlinear waves under certain conditions. Yin in [26] investigated the transitions and mechanisms of nonlinear waves in the (2 + 1)-dimensional Sawada-Kotera equation using characteristic lines and phase shift analysis, focusing on the dynamics of transformed waves. Chowdury [27] analyzed a quintic integrable equation of the nonlinear Schrödinger hierarchy, demonstrating how a breather solution can transform into a non-pulsating soliton solution.

In this paper, starting with an examination of relative positions of the characteristic lines, we consider the conditions under which the first-order and second-order breather solutions of the BLMP Equation (1.1) can transformed into other nonlinear waves and explore their localization and oscillatory behavior. According to the Hirota bilinear method, we obtain the 2-solitary wave and the 4-solitary wave solution [28]

$$u_2 = -2\left[\ln f_2\right]_x + u_0 y, \quad f_2 = 1 + \mathrm{e}^{\eta_1} + \mathrm{e}^{\eta_2} + A_{12}\mathrm{e}^{\eta_1+\eta_2}, \tag{1.5}$$

$$u_4 = -2\left[\ln f_4\right]_x + u_0 y, \quad f_4 = \sum_{\kappa=0,1} \exp\left(\sum_{i=1}^{4} \kappa_i \eta_i + \sum_{ij}^{4} \kappa_i \kappa_j A_{ij}\right), \tag{1.6}$$

where

$$\eta_i = k_i x + p_i y + \omega_i t + \phi_i, \quad \omega_i = \frac{3u_0 k_i^2}{p_i} - k_i^3, \quad i = 1,2,3,4, \tag{1.7}$$

$$\mathrm{e}^{A_{ij}} = \frac{u_0\left(k_i p_j - k_j p_i\right)^2 + k_i k_j p_i p_j \left(k_i - k_j\right)\left(p_i - p_j\right)}{u_0\left(k_i p_j - k_j p_i\right)^2 + k_i k_j p_i p_j \left(k_i + k_j\right)\left(p_i + p_j\right)}, \quad 1 \le i < j \le 4, \tag{1.8}$$

and k_i, p_i, ϕ_i are arbitrary constants, u_0 is a nonzero constant, $\sum_{\kappa=0,1}$ is the summation with all possible combinations of κ_i, $\kappa_j = 0,1$.

The structure of this paper is as follows. In Section 2, we first provide a detailed expression for the first-order breather and obtain the corresponding two characteristic lines. Various nonlinear transformed waves are obtained by controlling the relationships between the characteristic lines and adjusting the parameters. In Section 3, three types of transformation phenomena including non-transformed, semi-transformed and full-transformed are discussed. In Section 4, we present some conclusions.

2. State Transformation of the First-Order Breather Solution

In this section, starting with the 2-solitary wave solution and by taking the complex conjugate of the parameters, we derive the first-order breather solution of the (2 + 1)-dimensional BLMP Equation (1.1) and analyze its transformation mechanism. Firstly, taking

$$k_1 = \alpha_1 + \mathrm{i}\beta_1 = k_2^*, \quad p_1 = \nu_1 + \mathrm{i}\sigma_1 = p_2^*, \quad \phi_1 = \xi_1 + \mathrm{i}\mu_1 = \phi_2^*, \tag{2.1}$$

in f_2 defined by (1.5), where $*$ denotes the complex conjugate, α_1, β_1, ν_1, σ_1, ξ_1 and μ_1 are arbitrary real constants. Then f_2 can be rewritten as

$$f_2 = 2\mathrm{e}^{\Lambda_1}\left[\sqrt{M_1}\cosh\left(\Lambda_1 + \ln\sqrt{M_1}\right) + \cos\Gamma_1\right], \tag{2.2}$$

where

$$\Lambda_1 = \alpha_1 x + \nu_1 y + \omega_{1R} t + \xi_1, \quad \Gamma_1 = \beta_1 x + \sigma_1 y + \omega_{1I} t + \mu_1, \tag{2.3}$$

$$M_1 = \frac{u_0\left(\beta_1\nu_1 - \alpha_1\sigma_1\right)^2 + \beta_1\sigma_1\left(\alpha_1^2 + \beta_1^2\right)\left(\sigma_1^2 + \nu_1^2\right)}{u_0\left(\beta_1\nu_1 - \alpha_1\sigma_1\right)^2 - \alpha_1\nu_1\left(\alpha_1^2 + \beta_1^2\right)\left(\sigma_1^2 + \nu_1^2\right)}, \tag{2.4}$$

$$\omega_{1R} = \frac{6\alpha_1\beta_1\sigma_1 u_0 + 3\alpha_1^2 u_0\nu_1 - 3\beta_1^2 u_0\nu_1 + 3\alpha_1\beta_1^2\nu_1^2 + 3\alpha_1\beta_1^2\sigma_1^2 - \alpha_1^3\nu_1^2 - \alpha_1^3\sigma_1^2}{\sigma_1^2 + \nu_1^2}, \tag{2.5}$$

$$\omega_{1I} = \frac{6\alpha_1\beta_1\nu_1 u_0 - 3\alpha_1^2 u_0\sigma_1 + 3\beta_1^2 u_0\sigma_1 - 3\alpha_1^2\beta_1\nu_1^2 - 3\alpha_1^2\beta_1\sigma_1^2 + \beta_1^3\nu_1^2 + \beta_1^3\sigma_1^2}{\sigma_1^2 + \nu_1^2}. \tag{2.6}$$

The ω_{1R} and ω_{1I} denote the real and imaginary parts of ω_1 respectively. By substituting (2.2) into u_2, which is defined by (1.5), the first-order breather solution takes the form

$$u_2 = \frac{-2\alpha_1\sqrt{M_1}\sinh\left(\Lambda_1 + \ln\sqrt{M_1}\right) + 2\beta_1\sin\Gamma_1}{\sqrt{M_1}\cosh\left(\Lambda_1 + \ln\sqrt{M_1}\right) + \cos\Gamma_1} - 2\alpha_1 + u_0 y. \tag{2.7}$$

From the above equation, a singularity arises in the solution when the denominator equals zero. Therefore, we require that $M_1 > 1$ in all cases. Furthermore, by the properties of hyperbolic functions, the extreme values of the equation move along the line $\Lambda_1 + \ln\sqrt{M_1} = 0$.

For the first-order breather solution 2.7), we take the parameters

$$\alpha_1 = 3, \quad \beta_1 = 2, \quad \nu_1 = 1, \quad \sigma_1 = -2, \quad \xi_1 = 1, \quad \mu_1 = 1, \quad u_0 = 1. \tag{2.8}$$

The graph shows that the distance between adjacent peaks is uniform. In each periodic module, the single breather waveform has a main peak and two valleys, resembling a single lump. Therefore, it can also be viewed as an arrangement of multiple lump waves. In addition, the movement of the breather wave along the line $3x + y - \frac{12}{5}t + 1 + \frac{1}{2}\ln\frac{196}{131} = 0$ is periodic in the propagation direction and decays exponentially in the perpendicular direction.

By analyzing the solution, we can draw the following conclusions about the first-order breather: the first-order breather solution (15) consists of hyperbolic and trigonometric functions from which some properties of the solution can be determined. The hyperbolic functions $\sinh\left(\Lambda_1 + \ln\sqrt{M_1}\right)$ and $\cosh\left(\Lambda_1 + \ln\sqrt{M_1}\right)$ determine the local properties of the breather, while its periodicity is determined by the trigonometric function $\sin\Gamma_1$ and $\cos\Gamma_1$. Consequently, the nonlinear wave structure can be viewed as a superposition of two wave solutions: a solitary wave governed by Λ_1 and a periodic wave governed by Γ_1.

From the first-order breather solution (2.7), we notice that it has two key characteristic lines L_1 and L_2:

$$L_1 : \alpha_1 x + \nu_1 y + \omega_{1R} t + \ln\sqrt{M_1} + \xi_1 = 0, \tag{2.9}$$

$$L_2 : \beta_1 x + \sigma_1 y + \omega_{1I} t + \mu_1 = 0, \tag{2.10}$$

where the characteristic line L_1 determines the direction of movement. Then, by adjusting the parameter α_1, β_1, ν_1, σ_1, ξ_1 and μ_1, we consider the phenomena arising from the transformation of the first-order breather state when the two characteristic lines are parallel or non-parallel in the xOt plane.

The characteristic lines L_1 and L_2 are parallel in the xOt plane if and only if

$$\frac{\alpha_1}{\beta_1} = \frac{\omega_{1R}}{\omega_{1I}} \Leftrightarrow \begin{vmatrix} \alpha_1 & \omega_{1R} \\ \beta_1 & \omega_{1I} \end{vmatrix} = 0. \tag{2.11}$$

In the following, we will explore the transformation mechanism of the first-order breather based on the above conditions. It is important to emphasize that ensuring the non-singularity of the solution is a critical requirement, and it is necessary to require $M_1 > 1$ in all cases.

(i) If the relation between L_1 and L_2 satisfies $\begin{vmatrix} \alpha_1 & \omega_{1R} \\ \beta_1 & \omega_{1I} \end{vmatrix} \neq 0$, *i.e.*, L_1 and L_2 are not parallel in xOt plane, we can obtain the first-order breather where no transformation occurs in Figure 1.

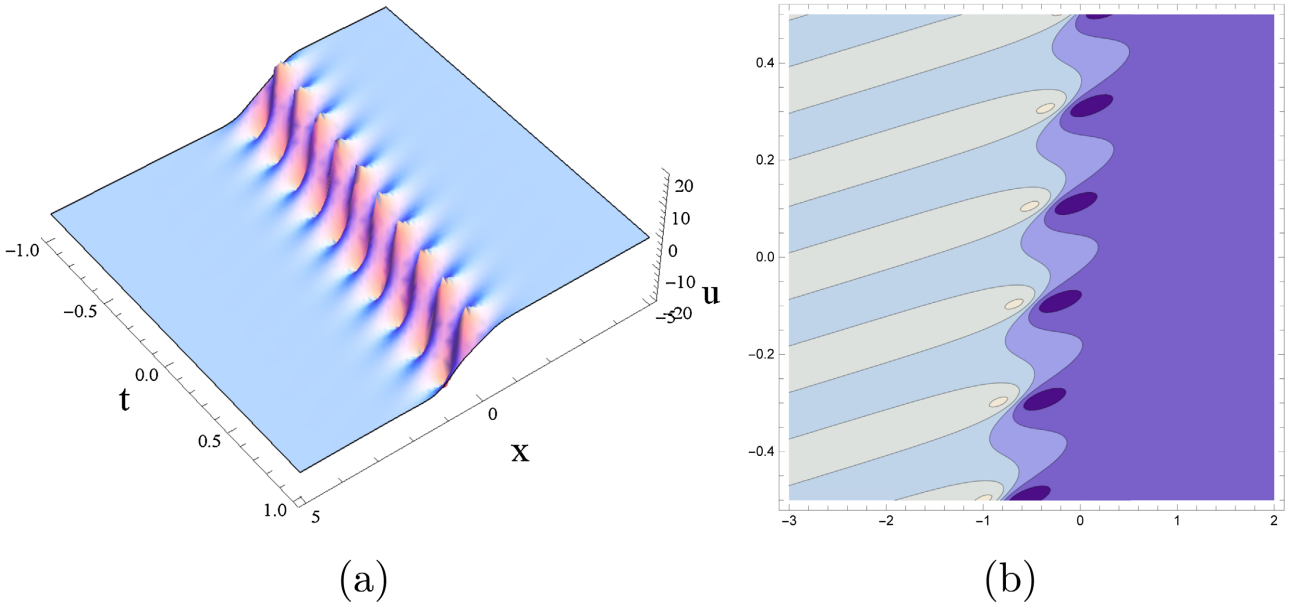

Figure 1. The first-order breather (2.7) with (2.8) at $y = 0$.

(ii) If the relation between L_1 and L_2 satisfies $\begin{vmatrix} \alpha_1 & \omega_{1R} \\ \beta_1 & \omega_{1I} \end{vmatrix} = 0$, *i.e.*, L_1 and L_2 are parallel in xOt plane. In this situation, we have

$$\beta_1 = \frac{3u_0\alpha_1\sigma_1}{3u_0\nu_1 - 2\nu_1^2\alpha_1 - 2\alpha_1\sigma_1^2}, \tag{2.12}$$

and the first-order breather can be transformed into various nonlinear waves by choosing different parameter relations.

Taking parameters with

$$u_0 = 1, \quad \alpha_1 = 1, \quad \nu_1 = 1, \quad \beta_1 = \frac{9}{17}, \quad \sigma_1 = -3, \quad \xi_1 = 1, \quad \mu_1 = 1, \tag{2.13}$$

in (2.7) as shown in Figure 2(a) and Figure 2(b) where $\left|\frac{\beta_1}{\alpha_1}\right| = \left|\frac{\omega_{1I}}{\omega_{1R}}\right| = \frac{9}{17}$. The figure illustrates a kink solitary wave converted from the first-order breather. In this case, the solution maintains the characteristics of a solitary wave, without exhibiting oscillatory or periodic behavior.

Taking parameters with

$$u_0 = 1, \quad \alpha_1 = \frac{7}{10}, \quad \nu_1 = 2, \quad \beta_1 = \frac{21}{26}, \quad \sigma_1 = -2, \quad \xi_1 = 1, \quad \mu_1 = 1, \tag{2.14}$$

in the (2.7) as shown in Figure 2(c) and Figure 2(d) where $\left|\frac{\beta_1}{\alpha_1}\right| = \left|\frac{\omega_{1I}}{\omega_{1R}}\right| = \frac{15}{13}$. We

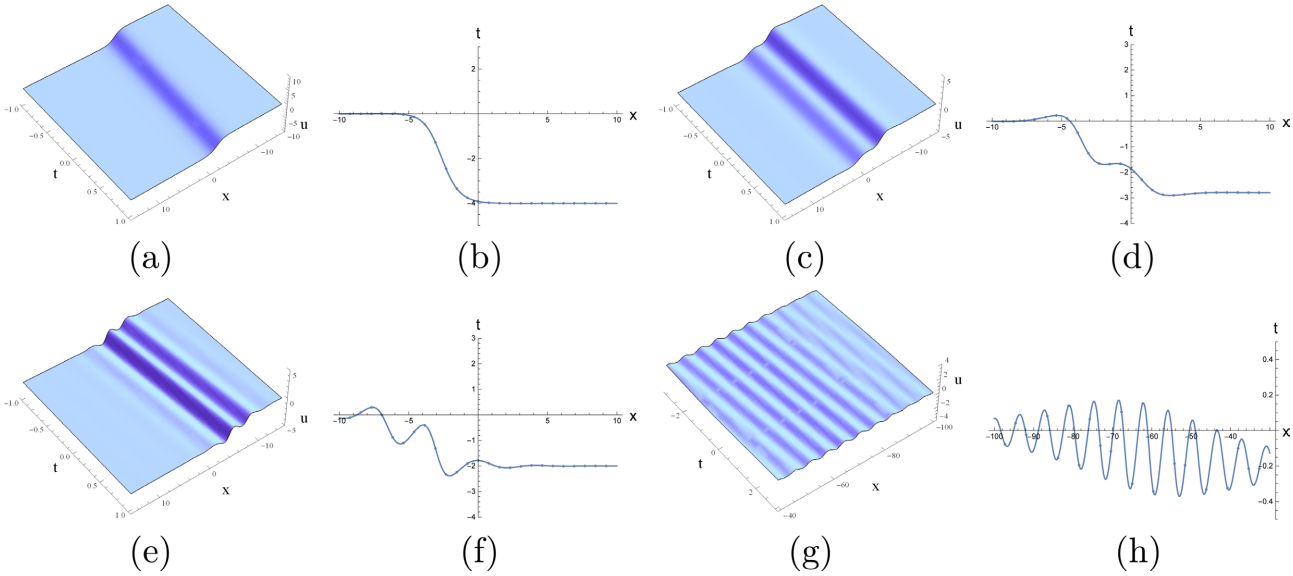

Figure 2. Transformation waves of the first-order breather (2.7) at $y=0$.

discover that the first-order breather can be transformed into *m*-shaped kink solitary wave in **Figure 2(c)**, which possesses two different wave peaks. In this paper, this structure is called *m*-kink type solitary wave.

Taking parameters with

$$u_0=1,\quad \alpha_1=\frac{1}{2},\quad \nu_1=2,\quad \beta_1=\frac{3}{2},\quad \sigma_1=-2,\quad \xi_1=1,\quad \mu_1=1, \tag{2.15}$$

in the (2.7) as shown in **Figure 2(e)** and **Figure 2(f)** where $\left|\frac{\beta_1}{\alpha_1}\right|=\left|\frac{\omega_{1I}}{\omega_{1R}}\right|=3$. The figure shows a multi-kink type solitary wave phenomenon with multiple peaks, where the periodicity becomes more apparent and the solitary wave characteristics weaken.

Taking parameters with

$$u_0=\frac{4}{63},\quad \alpha_1=\frac{1}{20},\quad \nu_1=1,\quad \beta_1=1,\quad \sigma_1=-1,\quad \xi_1=1,\quad \mu_1=1, \tag{2.16}$$

in the (2.7) as shown in **Figure 2(g)** and **Figure 2(h)** where $\left|\frac{\beta_1}{\alpha_1}\right|=\left|\frac{\omega_{1I}}{\omega_{1R}}\right|=20$. From the figure, it can be seen that the oscillation of wave is more apparent, and the peak value decreases. The first-order breather will be transformed into a periodic wave. As the ratio of $\left|\frac{\beta_1}{\alpha_1}\right|$ increases gradually, the periodicity of the breather becomes more and more obvious, and the solitary wave property almost disappears.

From the analysis above, we can observe that the solution (2.7) exhibits either dominant solitary wave characteristics with weak periodicity or dominant periodicity with weak solitary wave characteristics. Therefore, the first-order breather can be interpreted as a nonlinear superposition of solitary and periodic waves.

When the velocities of the two components are identical, the breather may transition into different types of nonlinear waves.

3. State Transformation of the Second-Order Breather Solution

In this section, we investigate the conversion mechanism of the second-order breather derived from f_4 defined by (1.6). Similarly, we select conjugate parameters to derive the second-order breather, and under specific parameter constraints, the breathers undergo partial or complete transformation.

The parameters k_1, k_2, p_1, p_2, ϕ_1 and ϕ_2 defined by (2.1) and we take

$$k_3 = \alpha_2 + \mathrm{i}\beta_2 = k_4^*, \quad p_3 = \nu_2 + \mathrm{i}\sigma_2 = p_4^*, \quad \phi_3 = \xi_2 + \mathrm{i}\mu_2 = \phi_4^*, \tag{3.1}$$

in f_4 defined by (1.6), where α_2, β_2, ν_2, σ_2, ξ_2 and μ_2 are arbitrary real constants.

Then f_4 can be rewritten as

$$\begin{aligned} f_4 = {} & 1 + 2\mathrm{e}^{\Lambda_1}\cos\Gamma_1 + 2\mathrm{e}^{\Lambda_2}\cos\Gamma_2 + M_1\mathrm{e}^{2\Lambda_1} + M_2\mathrm{e}^{2\Lambda_2} + M_1M_2\mathrm{e}^{2(\Lambda_1+\Lambda_2+b_1+b_2)} \\ & + 2\mathrm{e}^{\Lambda_1+\Lambda_2+b_1}\cos\left(\Gamma_1+\Gamma_2+a_1\right) + 2\mathrm{e}^{\Lambda_1+\Lambda_2+b_2}\cos\left(\Gamma_1-\Gamma_2+a_2\right) \\ & + 2M_1\mathrm{e}^{2\Lambda_1+\Lambda_2+b_1+b_2}\cos\left(\Gamma_2+a_1-a_2\right) + 2M_2\mathrm{e}^{\Lambda_1+2\Lambda_2+b_1+b_2}\cos\left(\Gamma_1+a_1+a_2\right), \end{aligned} \tag{3.2}$$

where Λ_1, Γ_1 and M_1 are defined by (2.3)-(3.6), in addition

$$b_1 = \ln\sqrt{\left(\mathrm{Re}\,A_{13}\right)^2 + \left(\mathrm{Im}\,A_{13}\right)^2}, \quad a_1 = \arctan\frac{\mathrm{Im}\,A_{13}}{\mathrm{Re}\,A_{13}}, \tag{3.3}$$

$$b_2 = \ln\sqrt{\left(\mathrm{Re}\,A_{14}\right)^2 + \left(\mathrm{Im}\,A_{14}\right)^2}, \quad a_2 = \arctan\frac{\mathrm{Im}\,A_{14}}{\mathrm{Re}\,A_{14}}, \tag{3.4}$$

$$M_2 = \frac{u_0\left(\beta_2\nu_2 - \alpha_2\sigma_2\right)^2 + \beta_2\sigma_2\left(\alpha_2^2+\beta_2^2\right)\left(\sigma_2^2+\nu_2^2\right)}{u_0\left(\beta_2\nu_2 - \alpha_2\sigma_2\right)^2 - \alpha_2\nu_2\left(\alpha_2^2+\beta_2^2\right)\left(\sigma_2^2+\nu_2^2\right)}, \tag{3.5}$$

$$\Lambda_2 = \alpha_2 x + \nu_2 y + \omega_{2R}t + \xi_2, \quad \Gamma_2 = \beta_2 x + \sigma_2 y + \omega_{2I}t + \mu_2, \tag{3.6}$$

$$\omega_{2R} = \frac{6\alpha_2\beta_2\sigma_2u_0 + 3\alpha_2^2u_0\nu_2 - 3\beta_2^2u_0\nu_2 + 3\alpha_2\beta_2^2\nu_2^2 + 3\alpha_2\beta_2^2\sigma_2^2 - \alpha_2^3\nu_2^2 - \alpha_2^3\sigma_2^2}{\sigma_2^2+\nu_2^2}, \tag{3.7}$$

$$\omega_{2I} = \frac{6\alpha_2\beta_2\nu_2u_0 - 3\alpha_2^2u_0\sigma_2 + 3\beta_2^2u_0\sigma_2 - 3\alpha_2^2\beta_2\nu_2^2 - 3\alpha_2^2\beta_2\sigma_2^2 + \beta_2^3\nu_2^2 + \beta_2^3\sigma_2^2}{\sigma_2^2+\nu_2^2}. \tag{3.8}$$

We can obtain the second-order breather solution by combining the transformations (1.2). Then we analyze its asymptotic properties in xOt plane to understand the nature of this solution. Without loss of generality, we assume

$$\alpha_1 > 0, \quad \alpha_2 > 0, \quad \frac{\omega_{1R}}{\alpha_1} > \frac{\omega_{2R}}{\alpha_2}. \tag{3.9}$$

Before collision ($t \to -\infty$):

(a) Fixing Λ_1, one can obtain $\Lambda_2 \to +\infty$, then

$$f_4 = 2\mathrm{e}^{\Lambda_1+b_1+b_2}\left[\sqrt{M_1}\cosh\left(\Lambda_1+b_1+b_2+\ln M_1\right) + \cos\left(\Gamma_1+a_1+a_2\right)\right], \tag{3.10}$$

and

$$u \sim u_{\Lambda_1}^{-}, \quad u_{\Lambda_1}^{-} = \frac{-2\alpha_1\sqrt{M_1}\sinh\left(\Lambda_1 + b_1 + b_2 + \ln\sqrt{M_1}\right) + 2\beta_1\sin\left(\Gamma_1 + a_1 + a_2\right)}{\sqrt{M_1}\cosh\left(\Lambda_1 + b_1 + b_2 + \ln\sqrt{M_1}\right) + \cos\left(\Gamma_1 + a_1 + a_2\right)} - 2\alpha_1 + u_\vartheta y. \tag{3.11}$$

(b) Fixing Λ_2, one can obtain $\Lambda_1 \to -\infty$, then

$$f_4 = 2\mathrm{e}^{\Lambda_2}\left[\sqrt{M_2}\cosh\left(\Lambda_2 + \ln\sqrt{M_2}\right) + \cos\Gamma_2\right], \tag{3.12}$$

and

$$u \sim u_{\Lambda_2}^{-}, \quad u_{\Lambda_2}^{-} = \frac{-2\alpha_2\sqrt{M_2}\sinh\left(\Lambda_2 + \ln\sqrt{M_2}\right) + 2\beta_2\sin\Gamma_2}{\sqrt{M_2}\cosh\left(\Lambda_2 + \ln\sqrt{M_2}\right) + \cos\Gamma_2} - 2\alpha_2 + u_0 y. \tag{3.13}$$

After collision ($t \to +\infty$):

(c) Fixing Λ_1, one can obtain $\Lambda_2 \to -\infty$, then

$$f_4 = 2\mathrm{e}^{\Lambda_1}\left[\sqrt{M_1}\cosh\left(\Lambda_1 + \ln\sqrt{M_1}\right) + \cos\Gamma_1\right], \tag{3.14}$$

and

$$u \sim u_{\Lambda_1}^{+}, \quad u_{\Lambda_1}^{+} = \frac{-2\alpha_1\sqrt{M_1}\sinh\left(\Lambda_1 + \ln\sqrt{M_1}\right) + 2\beta_1\sin\Gamma_1}{\sqrt{M_1}\cosh\left(\Lambda_1 + \ln\sqrt{M_1}\right) + \cos\Gamma_1} - 2\alpha_1 + u_0 y. \tag{3.15}$$

(d) Fixing Λ_2, one can obtain $\Lambda_1 \to +\infty$, then

$$f_4 = 2\mathrm{e}^{\Lambda_2 + b_1 + b_2}\left[\sqrt{M_2}\cosh\left(\Lambda_2 + b_1 + b_2 + \ln M_2\right) + \cos\left(\Gamma_2 + a_1 - a_2\right)\right], \tag{3.16}$$

and

$$u \sim u_{\Lambda_2}^{+}, \quad u_{\Lambda_2}^{+} = \frac{-2\alpha_2\sqrt{M_2}\sinh\left(\Lambda_2 + b_1 + b_2 + \ln\sqrt{M_2}\right) + 2\beta_2\sin\left(\Gamma_2 + a_1 - a_2\right)}{\sqrt{M_2}\cosh\left(\Lambda_2 + b_1 + b_2 + \ln\sqrt{M_2}\right) + \cos\left(\Gamma_2 + a_1 - a_2\right)} - 2\alpha_2 + u_0 y. \tag{3.17}$$

The above analysis allows us to obtain an asymptotic expression for the solution defined by (1.2) and (3.2), namely

$$u \to \begin{cases} u_{\Lambda_1}^{-} + u_{\Lambda_2}^{-}, & t \to -\infty, \\ u_{\Lambda_1}^{+} + u_{\Lambda_2}^{+}, & t \to +\infty. \end{cases} \tag{3.18}$$

The second-order breather can be obtained in Figure 3 by taking

$$\begin{aligned} &u_0 = 1, \quad \alpha_1 = \frac{1}{2}, \quad \beta_1 = \frac{1}{2}, \quad \nu_1 = \frac{7}{12}, \quad \sigma_1 = \frac{1}{12}, \quad \xi_1 = 1, \quad \mu_1 = 0, \\ &\alpha_2 = \frac{1}{3}, \quad \beta_2 = \frac{1}{2}, \quad \nu_2 = \frac{5}{18}, \quad \sigma_2 = \frac{1}{18}, \quad \xi_2 = 1, \quad \mu_2 = 0, \end{aligned} \tag{3.19}$$

in (1.2) and (3.2). As can be seen from the figure, there is no transformation between breathers. According to the first-order transformation mechanism, the breather can be converted by controlling the characteristic lines. In this paper, the transformation of the second-order breather can be classified into non-transformed, semi-transformed and full-transformed according to the type of transformation.

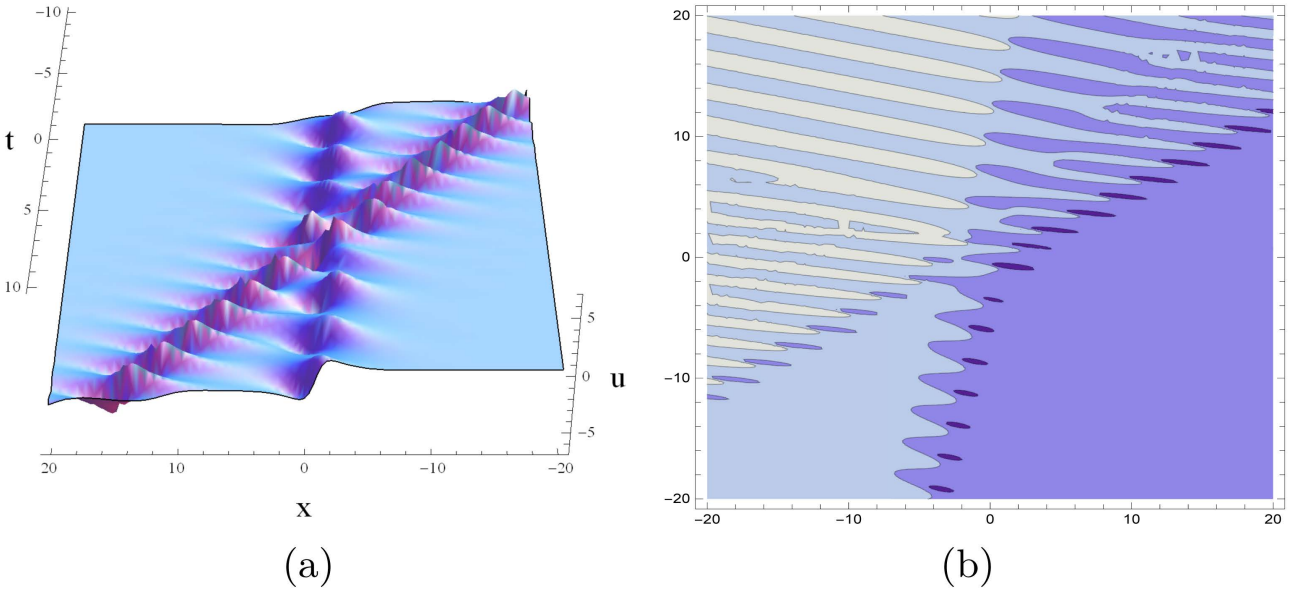

Figure 3. The second-order breather (1.2) and (3.2) with (3.19) at $y=0$.

In the following, the transformation of the second-order breather solution of the BLMP Equation (1.1) will be investigated based on the relationship between the two sets of characteristic lines in xOt plane. The second-order breather has two groups of characteristic lines L_1 and L_2 defined by (2.9) and (2.10) as well as L_3 and L_4:

$$L_3: \alpha_2 x + \nu_2 y + \omega_{2R} t + \ln\sqrt{M_2} + \xi_2 = 0, \tag{3.20}$$

$$L_4: \beta_2 x + \sigma_2 y + \omega_{2I} t + \mu_2 = 0. \tag{3.21}$$

Case I (Non-transformed): We suppose that L_1 and L_2 are not parallel, and L_3 and L_4 are not parallel which means that they satisfy

$$\begin{vmatrix} \alpha_1 & \omega_{1R} \\ \beta_1 & \omega_{1I} \end{vmatrix} \neq 0, \quad \begin{vmatrix} \alpha_2 & \omega_{2R} \\ \beta_2 & \omega_{2I} \end{vmatrix} \neq 0. \tag{3.22}$$

At this stage the two breathers collide elastically and neither transforms, as shown in Figure 3.

Case II (Semi-transformed): We suppose that L_1 and L_2 are not parallel, and L_3 and L_4 are parallel which means that they satisfy

$$\begin{vmatrix} \alpha_1 & \omega_{1R} \\ \beta_1 & \omega_{1I} \end{vmatrix} \neq 0, \quad \begin{vmatrix} \alpha_2 & \omega_{2R} \\ \beta_2 & \omega_{2I} \end{vmatrix} = 0. \tag{3.23}$$

One of the breathesr does not transform and the other one transforms into other nonlinear wave when the condition in the above is satisfied.

Taking parameters with

$$\begin{aligned} &u_0 = 1, \quad \alpha_1 = 1, \quad \beta_1 = 1, \quad \nu_1 = 1, \quad \sigma_1 = -3, \quad \xi_1 = 1, \quad \mu_1 = 0, \\ &\alpha_2 = 1, \quad \beta_2 = \frac{9}{17}, \quad \nu_2 = 1, \quad \sigma_2 = -3, \quad \xi_2 = 1, \quad \mu_2 = 0, \end{aligned} \tag{3.24}$$

in (1.2) and (3.2), the plots of the solution are shown in Figure 4(a) and Figure 4(b).

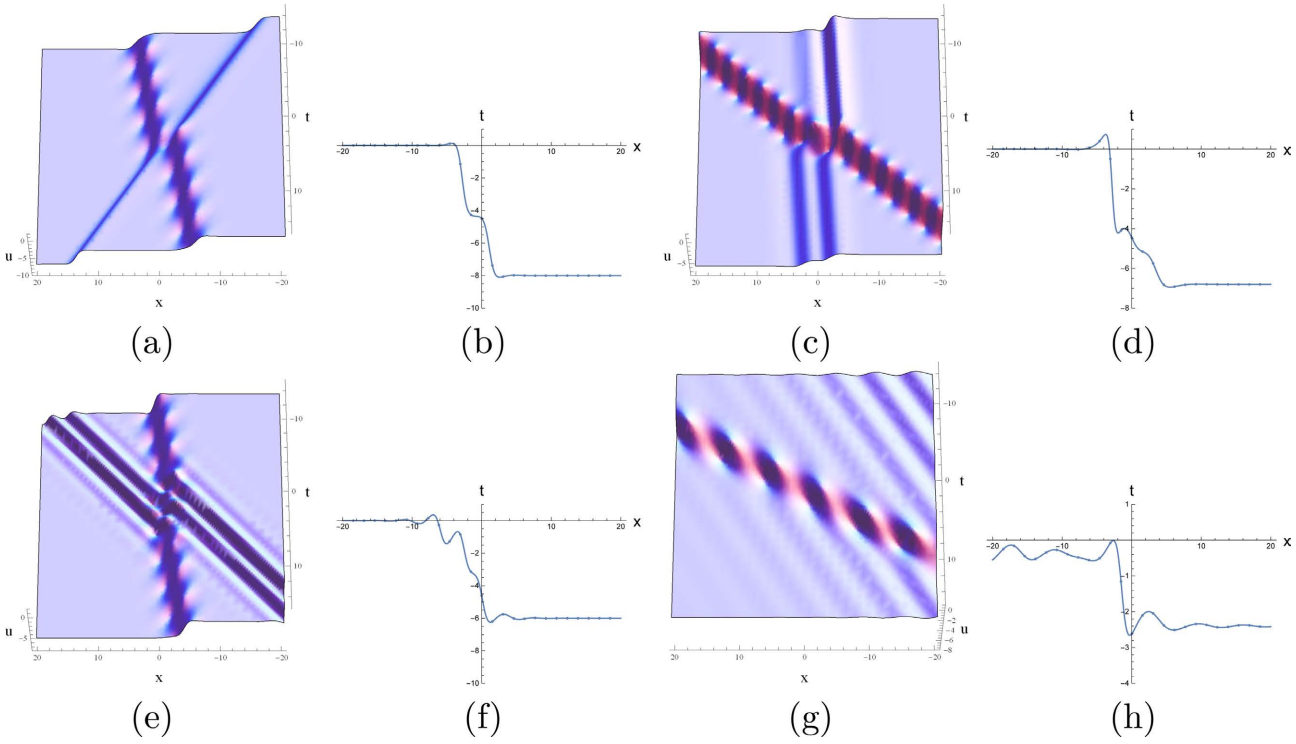

Figure 4. Semi-transformation waves of the second-order breather (1.2) with (3.2) at $y=0$.

The figures show the interaction of a breather and a kink solitary wave, describing the phenomenon that one of two breathers is a non-transformed wave and the other is transformed into a single kink solitary wave.

Taking parameters with

$$\begin{aligned} &u_0=1,\quad \alpha_1=1,\quad \beta_1=\frac{9}{7},\quad \nu_1=1,\quad \sigma_1=-3,\quad \xi_1=1,\quad \mu_1=0,\\ &\alpha_2=\frac{7}{10},\quad \beta_2=\frac{21}{26},\quad \nu_2=2,\quad \sigma_2=-2,\quad \xi_2=1,\quad \mu_2=0, \end{aligned} \tag{3.25}$$

in (1.2) and (3.2), the plots of the solution are illustrated in **Figure 4(c)** and **Figure 4(d)**. The figures represent the elastic interaction between the breather and the m-type kink solitary wave, and the phase shift of the two kink solitary waves is relatively obvious.

Taking parameters with

$$\begin{aligned} &u_0=1,\quad \alpha_1=1,\quad \beta_1=1,\quad \nu_1=1,\quad \sigma_1=-3,\quad \xi_1=1,\quad \mu_1=0,\\ &\alpha_2=\frac{1}{2},\quad \beta_2=\frac{3}{2},\quad \nu_2=2,\quad \sigma_2=-2,\quad \xi_2=1,\quad \mu_2=0, \end{aligned} \tag{3.26}$$

in (1.2) and (3.2), the plots of the solution are displayed in **Figure 4(e)** and **Figure 4(f)**. The figures demonstrate the interaction of a breather with a multi-kink solitary wave, namely, one breather does not transform and the other transforms into a multi-peak nonlinear wave.

Taking parameters with

$$\begin{aligned} &u_0 = \frac{4}{33}, \quad \alpha_1 = \frac{1}{10}, \quad \beta_1 = 1, \quad \nu_1 = 1, \quad \sigma_1 = -1, \quad \xi_1 = 1, \quad \mu_1 = 0, \\ &\alpha_2 = \frac{1}{10}, \quad \beta_2 = 1, \quad \nu_2 = 1, \quad \sigma_2 = -2, \quad \xi_2 = 1, \quad \mu_2 = 0, \end{aligned} \tag{3.27}$$

in (1.2) and (3.2), the plots of the solution are shown in Figure 4(g) and Figure 4(h). The figures show the phenomenon of the interaction between a breather and a periodic wave, and we can learn that by controlling the parameters we can make the periodicity of the transformed nonlinear wave more and more apparent.

Case III (Full-transformed): Supposing that L_1 and L_2 are parallel, as well as L_3 and L_4 are parallel which means that they satisfy

$$\begin{vmatrix} \alpha_1 & \omega_{1R} \\ \beta_1 & \omega_{1I} \end{vmatrix} = 0, \quad \begin{vmatrix} \alpha_2 & \omega_{2R} \\ \beta_2 & \omega_{2I} \end{vmatrix} = 0. \tag{3.28}$$

At this stage, both breathers experience transformation. Under certain parameter conditions each breather can be transformed into a different type of nonlinear wave, thus making the phenomenon more abundant.

Taking parameters with

$$\begin{aligned} &u_0 = 1, \quad \alpha_1 = 1, \quad \beta_1 = \frac{9}{17}, \quad \nu_1 = 1, \quad \sigma_1 = -3, \quad \xi_1 = 1, \quad \mu_1 = 0, \\ &\alpha_2 = \frac{7}{10}, \quad \beta_2 = \frac{21}{26}, \quad \nu_2 = 2, \quad \sigma_2 = -2, \quad \xi_2 = 1, \quad \mu_2 = 0, \end{aligned} \tag{3.29}$$

the plots of transformed nonlinear wave interactions are given by (1.2) with (3.2) in Figure 5(a) and Figure 5(b). The figures describe the transformation of one of two breathers into a single kink solitary wave and the other into an m-type kink solitary wave.

Taking parameters with

$$\begin{aligned} &u_0 = 1, \quad \alpha_1 = 1, \quad \beta_1 = \frac{9}{17}, \quad \nu_1 = 1, \quad \sigma_1 = -3, \quad \xi_1 = 1, \quad \mu_1 = 0, \\ &\alpha_2 = \frac{1}{2}, \quad \beta_2 = \frac{3}{2}, \quad \nu_2 = 2, \quad \sigma_2 = -2, \quad \xi_2 = 1, \quad \mu_2 = 0, \end{aligned} \tag{3.30}$$

the images of transformed nonlinear wave interactions are presented by (1.2) with (3.2) in Figure 5(c) and Figure 5(d). Similar to the previous case, the figures depict the transformation of one of the two breathers into a single kink solitary wave and the other into a multi-kink solitary wave.

Taking parameters with

$$\begin{aligned} &u_0 = 1, \quad \alpha_1 = \frac{7}{10}, \quad \beta_1 = \frac{21}{26}, \quad \nu_1 = 2, \quad \sigma_1 = -2, \quad \xi_1 = 1, \quad \mu_1 = 0, \\ &\alpha_2 = \frac{1}{2}, \quad \beta_2 = \frac{3}{2}, \quad \nu_2 = 2, \quad \sigma_2 = -2, \quad \xi_2 = 1, \quad \mu_2 = 0, \end{aligned} \tag{3.31}$$

in Equations (1.2) with (3.2), the plots of the solution are illustrated in Figure 5(e) and Figure 5(f). One breather transforms into an m-type kink solitary wave, while the other transforms into a multi-kink solitary wave.

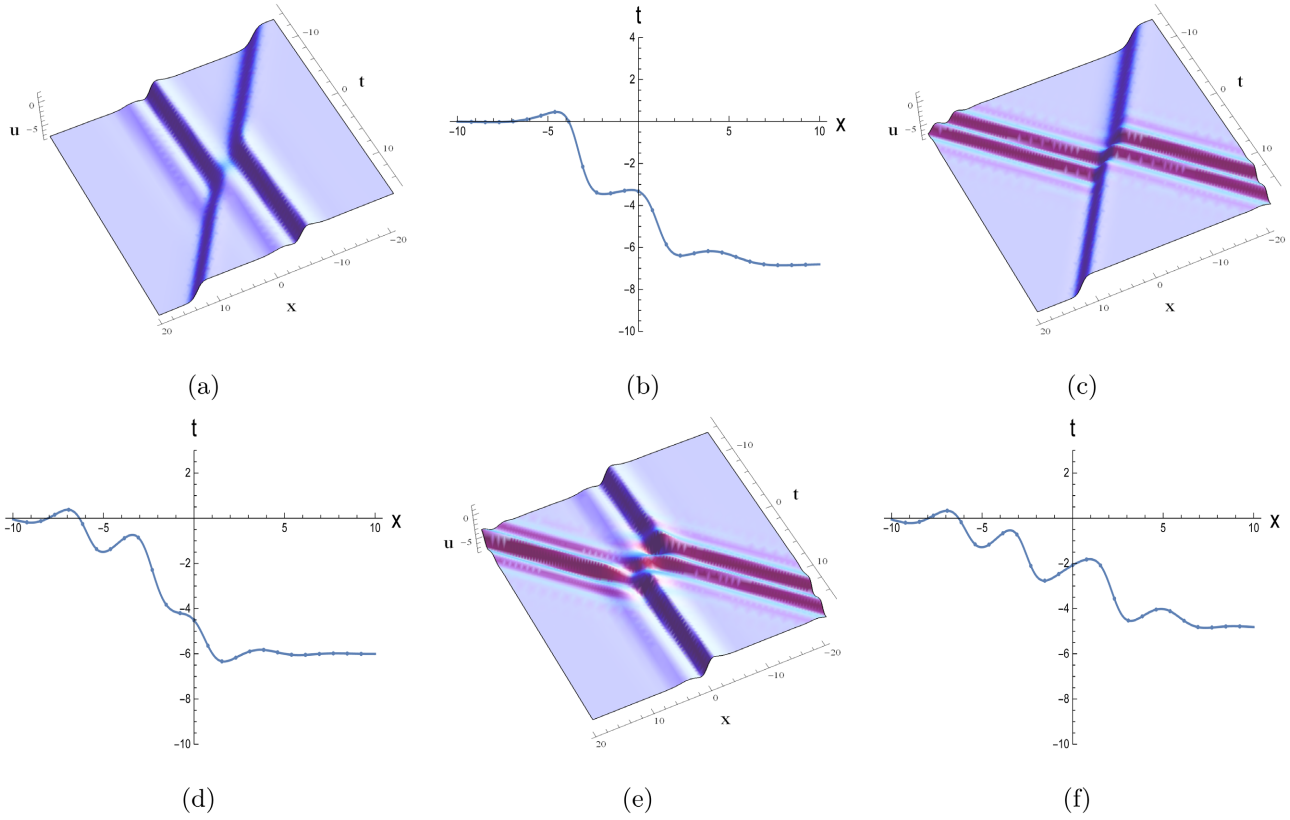

Figure 5. Full-transformation waves of the second-order breather (1.2) with (3.2).

4. Conclusion

In this paper, by means of the Hirota bilinear method, we obtain the first-order and the second-order breather from the two-solitary wave solution and four-solitary wave solution of the (2 + 1)-dimensional Boiti-Leon-Manna-Pempinelli equation, respectively. Based on the solution expressions, the exact solutions consist of hyperbolic and trigonometric functions, where the hyperbolic function represents a solitary wave, and the periodic wave describes a trigonometric function. The transformation mechanism of the first-order and second-order breathers presented in this paper primarily depends on adjusting the parameters and controlling the characteristic lines of the breathers. For different characteristic lines, several types of nonlinear waves in the xOt plane are illustrated, including kink solitary waves, m-kink type solitary waves, multi-kink type solitary waves and periodic waves. The periodic features of the transformed nonlinear waves become evident with the slope of the characteristic lines.

Conflicts of Interest

The author declares no conflicts of interest regarding the publication of this paper.

References

[1] Akram, S., Ahmad, J., Shafqat-Ur-Rehman, Alkarni, S. and Shah, N.A. (2023) Anal-

ysis of Lump Solutions and Modulation Instability to Fractional Complex Ginzburg-Landau Equation Arise in Optical Fibers. *Results in Physics*, **53**, Article 106991. https://doi.org/10.1016/j.rinp.2023.106991

[2] Younas, U. and Ren, J. (2023) Diversity of Wave Structures to the Conformable Fractional Dynamical Model. *Journal of Ocean Engineering and Science*, **8**, 559-572. https://doi.org/10.1016/j.joes.2022.04.014

[3] Siddig, A., Guo, Z., Zhou, Z. and Wu, B. (2018) An Image Denoising Model Based on a Fourth-Order Nonlinear Partial Differential Equation. *Computers & Mathematics with Applications*, **76**, 1056-1074. https://doi.org/10.1016/j.camwa.2018.05.040

[4] Kumar, S., Mohan, B. and Kumar, R. (2022) Lump, Soliton, and Interaction Solutions to a Generalized Two-Mode Higher-Order Nonlinear Evolution Equation in Plasma Physics. *Nonlinear Dynamics*, **110**, 693-704. https://doi.org/10.1007/s11071-022-07647-5

[5] Sang, X., Dong, H., Fang, Y., Liu, M. and Kong, Y. (2024) Soliton, Breather and Rogue Wave Solutions of the Nonlinear Schrödinger Equation via Darboux Transformation on a Time-Space Scale. *Chaos, Solitons & Fractals*, **184**, Article 115052. https://doi.org/10.1016/j.chaos.2024.115052

[6] Chen, H. and Zheng, S. (2023) Darboux Transformation for Nonlinear Schrödinger Type Hierarchies. *Physica D: Nonlinear Phenomena*, **454**, Article 133863. https://doi.org/10.1016/j.physd.2023.133863

[7] Zhang, Y. and Dong, H. (2022) Robust Inverse Scattering Method to the Complex Modified Korteweg-de Vries Equation with Nonzero Background Condition. *Physics Letters A*, **449**, Article 128359. https://doi.org/10.1016/j.physleta.2022.128359

[8] Ali, M.R., Khattab, M.A. and Mabrouk, S.M. (2023) Optical Soliton Solutions for the Integrable Lakshmanan-Porsezian-Daniel Equation via the Inverse Scattering Transformation Method with Applications. *Optik*, **272**, Article 170256. https://doi.org/10.1016/j.ijleo.2022.170256

[9] Ahmad, S., Saifullah, S., Khan, A. and Inc, M. (2022) New Local and Nonlocal Soliton Solutions of a Nonlocal Reverse Space-Time mKDV Equation Using Improved Hirota Bilinear Method. *Physics Letters A*, **450**, Article 128393. https://doi.org/10.1016/j.physleta.2022.128393

[10] Kumar, S. and Mohan, B. (2022) A Novel and Efficient Method for Obtaining Hirota's Bilinear Form for the Nonlinear Evolution Equation in (n+1) Dimensions. *Partial Differential Equations in Applied Mathematics*, **5**, Article 100274. https://doi.org/10.1016/j.padiff.2022.100274

[11] Yang, D. and Jiang, X. (2023) Line-Soliton, Lump and Interaction Solutions to the (2+1)-Dimensional Hirota-Satsuma-Ito Equation with Time-Dependent via Hirota Bilinear Forms. *Results in Physics*, **53**, Article 106904. https://doi.org/10.1016/j.rinp.2023.106904

[12] Ma, W. (2022) Soliton Solutions by Means of Hirota Bilinear Forms. *Partial Differential Equations in Applied Mathematics*, **5**, Article 100220. https://doi.org/10.1016/j.padiff.2021.100220

[13] Rabie, W.B., Ahmed, H.M., Darwish, A. and Hussein, H.H. (2023) Construction of New Solitons and Other Wave Solutions for a Concatenation Model Using Modified Extended Tanh-Function Method. *Alexandria Engineering Journal*, **74**, 445-451. https://doi.org/10.1016/j.aej.2023.05.046

[14] Zayed, E.M.E. and Al-Nowehy, A. (2017) The Solitary Wave Ansatz Method for Finding the Exact Bright and Dark Soliton Solutions of Two Nonlinear Schrödinger Equa-

tions. *Journal of the Association of Arab Universities for Basic and Applied Sciences*, **24**, 184-190. https://doi.org/10.1016/j.jaubas.2016.09.003

[15] Khalique, C.M. and Adeyemo, O.D. (2020) A Study of (3+1)-Dimensional Generalized Korteweg-de Vries-Zakharov-Kuznetsov Equation via Lie Symmetry Approach. *Results in Physics*, **18**, Article 103197. https://doi.org/10.1016/j.rinp.2020.103197

[16] Boiti, M., Leon, J.J.-P., Manna, M. and Pempinelli, F. (1986) On the Spectral Transform of a Korteweg-de Vries Equation in Two Spatial Dimensions. *Inverse Problems*, **2**, 271-279. https://doi.org/10.1088/0266-5611/2/3/005

[17] Wang, W., Bilige, S. and Shao, H. (2024) Superposition Formula of Arbitrary Functions to a (3+1)-Demensional Boiti-Leon-Manna-Pempinelli Equation. *Results in Physics*, **60**, Article 107641. https://doi.org/10.1016/j.rinp.2024.107641

[18] Kaplan, M. (2018) Two Different Systematic Techniques to Find Analytical Solutions of the (2+1)-Dimensional Boiti-Leon-Manna-Pempinelli Equation. *Chinese Journal of Physics*, **56**, 2523-2530. https://doi.org/10.1016/j.cjph.2018.06.005

[19] Mabrouk, S.M. and Rashed, A.S. (2017) Analysis of (3+1)-Dimensional Boiti-Leon-Manna-Pempinelli Equation via Lax Pair Investigation and Group Transformation Method. *Computers & Mathematics with Applications*, **74**, 2546-2556. https://doi.org/10.1016/j.camwa.2017.07.033

[20] Guo, C., Guo, Y., Wei, Z. and Gao, L. (2024) The New Kink Type and Non-Traveling Wave Solutions of (3+1)-Dimensional Boiti-Leon-Manna-Pempinelli Equation. *Alexandria Engineering Journal*, **96**, 34-41. https://doi.org/10.1016/j.aej.2024.03.090

[21] Li, L., Yan, Y. and Xie, Y. (2022) Variable Separation Solution for an Extended (3+1)-Dimensional Boiti-Leon-Manna-Pempinelli Equation. *Applied Mathematics Letters*, **132**, Article 108185. https://doi.org/10.1016/j.aml.2022.108185

[22] Lin, L. (2010) Quasi-Periodic Waves and Asymptotic Property for Boiti-Leon-Manna-Pempinelli Equation. *Communications in Theoretical Physics*, **54**, 208-214. https://doi.org/10.1088/0253-6102/54/2/02

[23] Chen, S., Yin, Y. and Lü, X. (2024) Elastic Collision between One Lump Wave and Multiple Stripe Waves of Nonlinear Evolution Equations. *Communications in Nonlinear Science and Numerical Simulation*, **130**, Article 107205. https://doi.org/10.1016/j.cnsns.2023.107205

[24] Wang, M., Chen, A. and Zhang, L. (2024) Elastic and Resonant Interactions of a Lump Wave and Solitary Waves for the (2+1)-Dimensional Ito Equation. *Results in Physics*, **58**, Article 107454. https://doi.org/10.1016/j.rinp.2024.107454

[25] Tajiri, M. and Watanabe, Y. (1997) Periodic Soliton Solutions as Imbricate Series of Rational Solitons: Solutions to the Kadomtsev-Petviashvili Equation with Positive Dispersion. *Journal of Nonlinear Mathematical Physics*, **4**, 350-357. https://doi.org/10.2991/jnmp.1997.4.3-4.9

[26] Yin, Z. and Tian, S. (2021) Nonlinear Wave Transitions and Their Mechanisms of (2+1)-Dimensional Sawada-Kotera Equation. *Physica D: Nonlinear Phenomena*, **427**, Article 133002. https://doi.org/10.1016/j.physd.2021.133002

[27] Chowdury, A., Kedziora, D.J., Ankiewicz, A. and Akhmediev, N. (2015) Breather-to-Soliton Conversions Described by the Quintic Equation of the Nonlinear Schrödinger Hierarchy. *Physical Review E*, **91**, Article 032928. https://doi.org/10.1103/physreve.91.032928

[28] Wazwaz, A. (2016) Multiple Kink Solutions for Two Coupled Integrable (2+1)-Dimensional Systems. *Applied Mathematics Letters*, **58**, 1-6. https://doi.org/10.1016/j.aml.2016.01.019